Dexamethasone Induces a Putative Repressor Complex and Chromatin Modifications in the CRH Promoter

Dharmendra Sharma, Shreyas Bhave, Elaine Gregg, and Rosalie Uht

Department of Pharmacology and Neuroscience (D.S., S.B., E.G., R.U.) and Institute for Aging and Alzheimer's Disease Research (D.S., E.G., R.U.), University of North Texas Health Science Center, Fort Worth, Texas

Glucocorticoids down-regulate expression of hypothalamic CRH; however, mechanisms by which they do so are not fully understood. The proximal promoter cAMP response element, negative glucocorticoid response element (nGRE), and methylated CpG islands all play a role in *crh* down-regulation. Dexamethasone (Dex)-repressed *crh* expression is associated with glucocorticoid receptor (GR) and histone deacetylase 1 (HDAC1) recruitment to the region of the *crh* promoter. Given that HDAC1 may be present in methylated CpG binding protein 2 (MeCP2) complexes, and that MeCP2 is known to play a role in regulating *crh* expression, we sought to determine whether or not HDAC1 and/or MeCP2 could interact with the GR. Dex enhanced GR interactions with both proteins. Glucocorticoid regulation of *crh* has also been associated with CpG methylation; thus we assessed whether GR could interact with a DNA methyltransferase (DnMT). Indeed, the GR interacted with DnMT3b, but not DnMT3a. In addition, Dex-induced occupancy of the *crh* promoter by HDAC1, MeCP2, and DnMT3b was associated with an increased level of promoter methylation, which appeared to be CpG site specific. Lastly, to extend previous assessment of chromatin modifications in this promoter region, the degree of histone methylation was measured. Dex increased trimethylation of histone 3-lysine 9, a marker of gene suppression; however, levels of di- and trimethylated histone 3-lysine 4, markers of gene activation, were not significantly changed. Taken together, the data suggest that Dex-mediated *crh* suppression involves formation of a repressor complex consisting of GR, MeCP2, and HDAC1, recruitment of DnMT3b, and associated changes in proximal promoter CpG methylation. **(*Molecular Endocrinology* 27: 1142–1152, 2013)**

The hypothalamic neuropeptide CRH plays a central role in regulation of stress responses. It is synthesized in the medial parvocellular region of the paraventricular nucleus of the hypothalamus and released into the pituitary portal circulation as an ACTH secretagogue (1, 2). Major regulators of *crh* expression consist of end products of the hypothalamic pituitary adrenal (HPA) axis itself, glucocorticoids. These steroids feed back to multiple sites in the central nervous system to regulate HPA axis activity (3). A major site of regulation is the paraventricular nucleus of the hypothalamus in which glucocorticoids decrease *crh* expression (4, 5).

Regulatory sites in *crh* include a cAMP response element (CRE) at −226 in rat and at −221 in humans (6, 7) and a negative glucocorticoid response element (nGRE) (8). The cAMP signaling pathway induces *crh* expression through activation of protein kinase A and subsequent recruitment of phosphorylated CRE binding protein (pCREB) to the *crh* promoter (6, 7, 9, 10). The mechanism of glucocorticoid-mediated down-regulation of *crh* expression involves glucocorticoid receptor (GR) binding to the nGRE (11) and recruitment of coregulatory molecules (12). This nGRE is a composite element that confers transcriptional regulation by GR, and activator protein 1 family members. In addition, activation via the CRE may

ISSN Print 0888-8809 ISSN Online 1944-9917
Printed in U.S.A.

Received March 28, 2013. Accepted May 8, 2013.
First Published Online May 13, 2013

Abbreviations: ChIP, chromatin immunoprecipitation; CRE, cAMP response element; Dex, dexamethasone; DnMT, DNA methyltransferase; GR, glucocorticoid receptor; HDAC, histone deacetylase; H3-K9, histone 3-lysine 9; HPA, hypothalamic pituitary adrenal; MeCP2, methylated CpG binding protein 2; nGRE, negative glucocorticoid response element; pCREB, phosphorylated CRE binding protein; PMSF, phenylmethylsulfonyl fluoride.

be blocked by the inducible cAMP repressor (Ref. 13 for review).

Chromatin modifications play a role in the regulation of countless genes. One mechanism of down-regulation involves methylation of CpG islands by DNA methyltransferases (DnMTs). This family of enzymes includes 3 members: DnMT1, DnMT3a, and DnMT3b. DnMT1 is involved in the maintenance of hemimethylated DNA whereas the DnMT 3a and 3b are involved in de novo methylation (Ref. 14 for review). DNA methylation leads to transcriptional repression by interfering with transcription factor binding (15) and/or by recruiting methylated DNA binding proteins, eg, methylated CpG binding protein 2 (MeCP2). MeCP2, in turn, is associated with histone deacetylase (HDAC) repressive machinery (16). The *crh* proximal promoter contains a number of CpG dinucleotides that are targets for MeCP2 binding (17) and have been shown to be associated with regulation of *crh* (17–19).

In addition to DNA methylation, methylation of histone H3 and H4 lysine residues are known to be involved in transcriptional regulation (20–23). However, there are no published reports of direct glucocorticoid-regulated histone methylation at the *crh* promoter, even though it is known that MeCP2 links DNA methylation to histone methylation (Ref. 24 for review).

The aim of the present study was to elucidate mechanisms by which glucocorticoid-bound GR (the GR holoreceptor) down-regulate the CRH gene (*crh*) expression via chromatin modifications. We asked whether dexamethasone (Dex)-bound GR could participate in a MeCP2-HDAC1 and/or DnMT complex and lead to increased promoter methylation. We also asked whether Dex-induced suppression of the *crh* promoter is associated with changes in the methylation levels of specific histone H3 lysine residues. For all of the experiments we used a rat hypothalamic neuronal cell line, IVB, which expresses CRH (25). The data presented suggest that the GR holoreceptor leads to the formation of a repressor complex consisting of GR-MeCP2-HDAC1 that is recruited to the region of the *crh* promoter. Furthermore, GR associates with DnMT3b, which in turn is associated with CpG site-specific increased methylation of the *crh* promoter. Lastly, the increase in promoter methylation correlates with an increase in histone H3 methylation, specifically trimethylation of histone 3-lysine 9 (H3-K9) a marker of transcriptional repression.

Materials and Methods

Cell culture and immunocytochemistry

Rat hypothalamic IVB cells (25), the only cells used in these experiments, were plated and grown in phenol red-free DMEM/Ham's F12 (Hyclone Laboratories, Logan, Utah), supplemented with 10% newborn calf serum (Gemini Bio-Products, West Sacramento, California); 100 U/mL penicillin/streptomycin; 0.1 mM nonessential amino acids; 1 mM sodium pyruvate; and 2 mM L-glutamine (Mediatech, Manassas, Virginia). For all studies, cells were incubated for 48 hours in a medium supplemented with charcoal-stripped serum and then treated with ethanol vehicle (Veh) or Dex (10^{-7}M) for 2 hours before collection.

Immunocytochemical analysis was performed using Lab-Tek II Chamber Slides (Nalge Nunc International, Rochester, New York). After fixation in 4% paraformaldehyde, cells were permealized with 0.1% Triton X-100. Nonspecific binding was blocked using a solution of 5% normal goat serum and 2% BSA in PBS. After blocking, cells were incubated overnight with primary antibodies (dilution 1:250) at 4°C. They were then washed with PBS and incubated with a 1:1000 dilution of a mixture of Alexa Fluor 594-goat antirabbit IgG and 488-goat antimouse (Molecular Probes, Eugene, Oregon; Invitrogen, Carlsbad, California) for 1 hour. After washing, cells were mounted in FluorSave reagent (Calbiochem, La Jolla, California). Images were captured with Nuance Multispectral Imaging System (Burlington, Massachusetts). Digitized images were arranged using Adobe Photoshop (Adobe Systems, San Jose, California).

RNA isolation and quantitative RT-PCR

Total RNA was isolated using Tri reagent (Molecular Research Center, Ohio). For reverse transcription, 1 μg of total RNA was used for cDNA synthesis, which was performed at 42°C for 30 minutes using the Verso cDNA kit (Thermo Fisher Scientific, Pittsburgh, Pennsylvania). Changes in the levels of CRH mRNA were measured by quantitative RT-PCR using IQ SYBR Green Super Mix (Bio-Rad Laboratories, Hercules, California) and 0.4 μM of each primer on a CFX96 Real-Time PCR detection system (Bio-Rad Laboratories). The primer sequences for the CRH mRNA are 5′-TGTCGCCCTGTCTGCCTTGC (forward) and 5′-AGCCGAGCAGCGGGACTTCT (reverse). Levels of glyceraldehyde-3-phosphate dehydrogenase mRNA were used to normalize data. Primers used to amplify glyceraldehyde-3-phosphate dehydrogenase are 5′-TGGAGTCTACTGGCGTCTT (forward) and 5′-GCTGACAATCTTGAGGGAG (reverse). Samples were amplified by an initial denaturation at 95°C for 3 minutes and then cycled (44×) using 95°C for 30 seconds, 60°C for 30 seconds, and 72°C for 60 seconds. For calculation of the real-time data the ΔΔCT method was used (26). A melt curve analysis was performed in each assay to ensure the amplification of a single product.

Protein sample preparation

For Western blot analysis cytoplasmic and nuclear extracts were prepared by the method adapted from Sadowski (27). Briefly, cells were washed with cold PBS and scraped in 500 μL of buffer A (10 mM HEPES pH 7.9, 10 mM KCL, 0.1 mM EDTA, 20 μL of 10% IGEPAL, 1 mM dithiothreitol, 1 mM phenylmethylsulfonyl fluoride [PMSF], and protease inhibitor cocktail). Lysate was centrifuged at 15 000 × *g* for 3 minutes to pellet nuclei. Nuclear pellets were resuspended by repeated pipeting in buffer B (20 mM HEPES [pH 7.9], 0.4 M NaCl, 1 mM EDTA, 10% glycerol, 1 mM dithiothreitol, 1 mM PMSF, and protease inhibitor Cocktail [Sigma Chemical Co, St Louis, Mis-

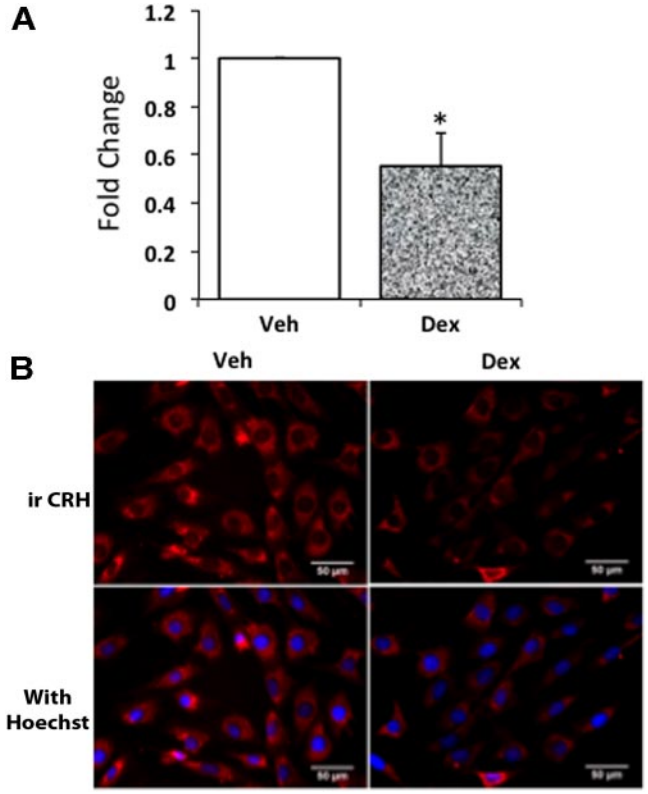

Figure 1. Dex Treatment Decreases the Expression of *crh* in IVB Cells. mRNA expression (panel A) and immunocytochemistry (ICC) (panel B). Cells were incubated in media containing stripped serum for 48 hours and then treated with Dex (10^{-7}M) for 2 hours. Expression of CRH mRNA was measured by real time RT-PCR (n = 3). Data represent mean ± SEM *, $P = .01$. ICC detection of CRH was performed with a polyclonal antibody (Abnova, Taipei, Taiwan) at a 1:250 dilution. ir, immunoreactivity; Veh, vehicle.

souri]). Samples were shaken vigorously at 4°C for 2 hours and then centrifuged at 15 000 × *g* for 5 minutes to remove debris.

Western blot analysis

Nuclear and cytoplasmic samples were boiled in Laemmli buffer for 10 minutes before electrophoresis. Western blots (28) were performed according to standard procedures. After transfer, polyvinylidene difluoride membranes (Bio-Rad Laboratories) were blocked and probed with the primary antibody (dilution 1:1000) as indicated in the figure legends. Horseradish peroxidase-conjugated goat antimouse IgG or antirabbit IgG (1:5000, Millipore Corp., Bedford, Massachusetts) were used as secondary antibodies. Proteins were visualized using Enhanced Chemiluminescent Substrate (Pierce Biotechnology, Inc., Rockford, Illinois). For densitometry analysis, bands were quantified by NIH Image J software.

Coimmunoprecipitation

After treatment, cells were washed once with cold PBS and whole-cell extract was prepared using CoIP lysis buffer (150 mM NaCl, 50 mM Tris-HCl [pH 7.4], 1% Igepal 630, 1 mM EDTA, 10% glycerol, 1 mM sodium orthovanadate, 1 mM sodium fluoride) supplemented with 1 mM PMSF and protease inhibitor cocktail. Six hundred micrograms of cell extract were incubated overnight at 4°C with 3 μL of primary antibody (1 μg/μL) followed by incubation with Protein A/G-coated agarose beads (Santa Cruz Biotechnology, Santa Cruz, California) for another 4 hours at 4°C. Samples were then washed 4 times with ice-cold immunoprecipitation lysis buffer and finally with PBS.

Chromatin immunoprecipitation (ChIP) and real-time PCR

For ChIP, cells at 80–90% confluency were used. They were treated with α-amanitin for 2 hours to synchronize the cell cycle. We have found that aminitin treatment decreases variability in the data when performing ChIPs that target the *crh* promoter (our unpublished data). Cells were washed twice with PBS, and then treated with ethanolic vehicle, or Dex (10^{-7} M) for 2 hours. ChIP was performed as described previously (29–31). Briefly, cells were fixed in 1% formaldehyde for 10 minutes at room temperature. Fixation was stopped by addition of glycine (0.125 M). After washing twice in ice-cold PBS, cells were scraped and centrifuged at 590 × *g* for 1 minute. Pellets were resuspended in 800 μL of cell sonication buffer (1% Triton X-100, 0.1% deoxycholate, 50 mM Tris [pH 8.1], 150 mM NaCl, 5 mM EDTA, 1 mM PMSF, and 10 μL/mL of protease inhibitor cocktail), incubated on ice for 10 minutes and subjected to sonication (Misonix sonicator Q700 with cup horn, QSonica, LLC, Newtown, Connecticut). Five 30-second pulses at 80% amplitude were used to shear chromatin to 400- to 1000-bp fragments. Samples were centrifuged at 16 000 × *g* for 15 minutes at 4°C. One hundred micrograms of total protein was diluted with cell sonication buffer to a final volume of 1.0 mL. Samples were incubated overnight with 3 μL of antibody (1 μg/μL) as described in the figure. Precipitation and washing of chromatin samples have been described (30). Finally, DNA was resuspended in 100 μL of TE buffer, pH 7.5. For real-time PCR, 5 μL of template DNA was used and amplified using SYBR green super mix (Bio-Rad Laboratories) and 0.4 μM of each primer. The primer sequences are 5′-TCAGTATGTTTTCCACACTTGGAT (forward) and 5′-TTTATCGCCTCCTTGGTGAC (reverse); they flank a region of *crh* that contains the proximal CRE, nGRE, and CpG islands. Real-time PCR values were calculated by the ΔΔCT method (26) and expressed as fold differences of vehicle. A melt curve analysis was performed each time to ensure that a single product was amplified. As a negative control, PCR primers were also designed to target upstream regions of the CRH promoter that do not have GR binding sites. These are *crh*-4000 −3441 TGCCATTGCTATTTGGCTGA −3421 (forward) and −3285 GGTGTCACAGCCATACATCCT −3264 (reverse); *crh*-3000: −2361 GTGCATCAGTGCACATCACA −2347 (forward) and: −2237 TGATGTGCCTTTTCTCCGGT −2217 (reverse); *crh*-2000: −1386 TACAGGTCCCAAACAGGGGT −1366 (forward) and: −1273 CAGTTGCCTCATAACCACCAC −1252 (reverse). Lastly, as a positive control, GR binding sites at the Per1 gene promoter were targeted. Primer pairs for the *Per1* promoter are: 5′-GGTCCAAAGACCCCCTTCAG (forward) and 5′-GTTCTTGCTGTTGGCCACAG (reverse).

Genomic DNA purification, sodium bisulfite treatment, and methylation analysis

To evaluate the level of CpG methylation in the *crh* proximal promoter, genomic DNA was extracted and purified using phe-

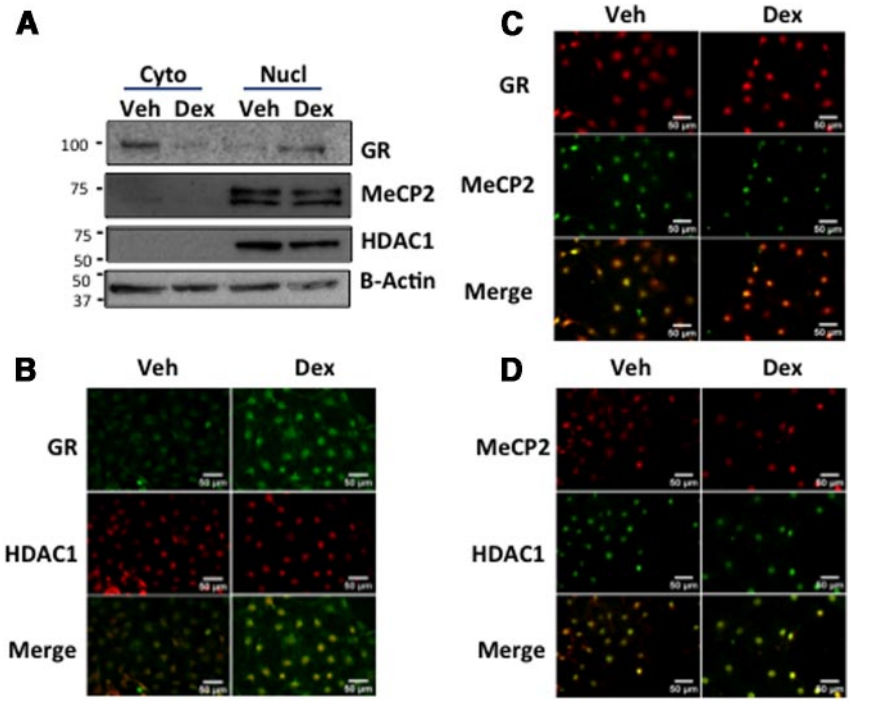

Figure 2. Localization of GR, MeCP2, and HDAC1. A, Western blot analysis of GR, MeCP2, and HDAC1. Cells were treated as described in Figure 1. Colocalization of GR and HDAC1 (B), GR and MeCP2 (C), and HDAC1 and MeCP2 (D). Antibodies used were as follows: B, monoclonal anti-GR (Thermo/Pierce) and polyclonal anti-HDAC1 (Abcam, Cambridge, Massachusetts); C, polyclonal anti-GR (Santa Cruz) and monoclonal MeCP2 (Sigma); D, polyclonal anti-MeCP2 (Abcam) and monoclonal anti-HDAC1 (Abcam). All the antibodies were used at 1:250 dilutions. Cyto, cytoplasmic; Nucl, nuclear; Veh, vehicle.

nol-chloroform. Genomic DNA (800 ng) was modified with bisulfite treatment using EpiTect Bisulphite Kit (QIAGEN, Chatsworth, California) according to the manufacturer's guidelines. Modified DNA (100 ng) was subjected to the first round of PCR amplification using outside primers (5′-TTTTTTTTGGTTTGTATTTGGTT [forward] and 5′-ACCTTTCCCCTTTCTCTTCAAT[reverse]). The protocol involved an initial denaturation at 95°C for 5 minutes, followed by 34 cycles of denaturation (95°C, 60 sec), annealing (50°C, 60 sec), and extension (72°C, 60 sec) with a final extension cycle (72°C, 10 min). PCR product (5 μL; 406 bp) was used as a template for the second round of PCR using nested primers (5′-AATTTTTGTTAATGGATAAGT [forward] and 5′-AACTCTAAATTTCTCCACACCA[reverse]). The 294-bp PCR product was purified and cloned into pCR4-TOPO vector using TOPO-TA Cloning Kit (Life Technologies, Gaithersburg, Maryland). A total of 21 recombinant clones from 3 independent experiments were sequenced. Sequence information was analyzed and methylation data were compiled using the BISMA software available online (http://biochem.jacobs-university.de/BDPC/BISMA).

Statistical analysis

Statistical significance was performed using an unpaired *t* test. Data are presented as the average ± SEM of the number of observations indicated in the figure legends. $P < .05$ was considered significant.

Results

Dex decreases CRH expression in IVB cells

Consistent with our previously reported work (12), Dex (10^{-7} M) treatment led to an approximate 50% decrease in mRNA levels after 2 hours (Figure 1A). As expected, CRH immunoreactivity decreased after 2 hours of incubation with Dex (Figure 1B). Thus, in our hands, this cell line serves as a suitable model for mechanistic analysis.

Characterization of nuclear/cytoplasmic distribution of GR, HDAC1, and MeCP2

Localization of GR, HDAC1, and MeCP2 was analyzed by Western blot and ICC. As expected, Dex exposure led to translocation of GR from cytoplasm to nucleus (Figure 2A). HDAC1 and MeCP2 were nuclear irrespective of treatment (Figure 2A). Western blot analysis of MeCP2 revealed 2 bands (Figure 2A). The MeCP2 gene is known to be alternatively spliced in humans (32, 33) and rats (34), and the bands are presumed to correspond to previously reported isoforms, ie, MeCP2-e1 and MeCp2-e2 (34, 35). Immunocytochemical (Figure 2, B and C) and Western blot data were consistent. As expected HDAC1 was nuclear. Of note, this localization is not always the case; HDAC1 has been reported in the cytoplasm (36). MeCP2 immunoreactivity was also nuclear and overlapped with HDAC1(Figure 2D).

Dex treatment induces the association of GR with HDAC1 and MeCP2

To determine the degree of GR association with HDAC1 or MeCP2, coimmunoprecipitation analyses were performed. These analyses revealed that Dex enhanced interactions of GR with HDAC1 and with MeCP2 (Figure 3, A and B, respectively). MeCP2 has been reported to interact with HDAC1 (16) and, given our previous finding that Dex treatment increases HDAC1 occupancy of the *crh* promoter (12), we sought to determine whether Dex would contribute to HDAC1 and MeCP2 interaction in our conditions. Dex significantly increased the interaction of MeCP2 and HDAC1 (Figure 3C). Thus, the data

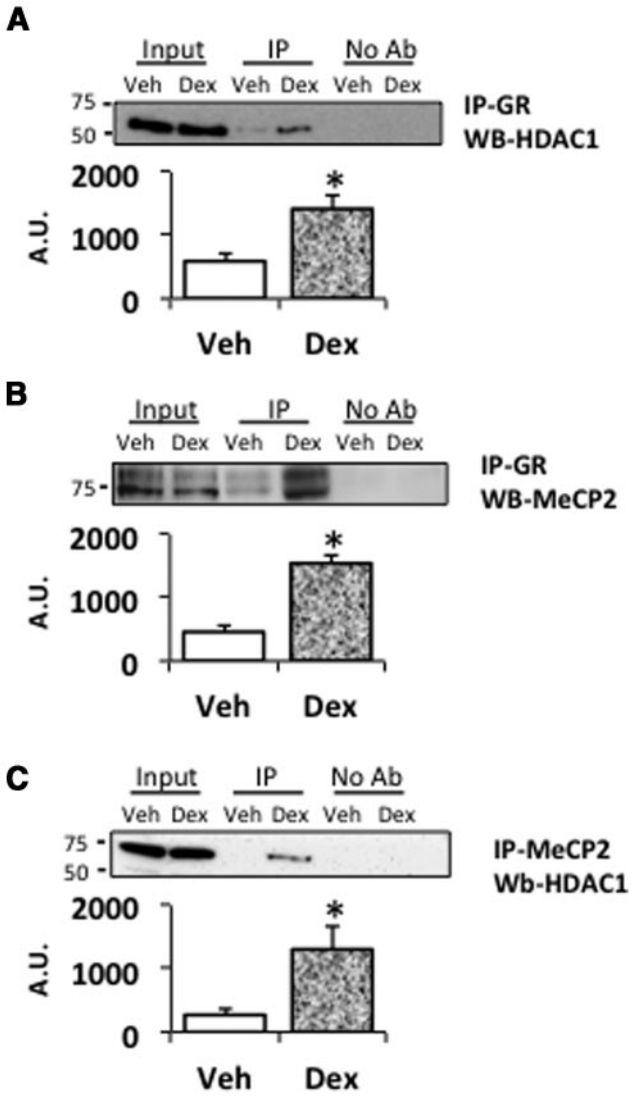

Figure 3. Dex Treatment Increases Association of GR with MeCP2 and HDAC1. Coimmunoprecipitation analysis of GR:HDAC1 (A), GR: MeCP2 (B), and MeCP2:HDAC1 (C). Cells were treated as indicated in the Figure 1 legend. Cell extracts were prepared and subjected to immunoprecipitation as indicated. Antibodies used were as follows: A, polyclonal GR (Santa Cruz) and monoclonal HDAC1 (Abcam); B, polyclonal GR (Santa Cruz) and monoclonal MeCP2 (Sigma); C, polyclonal MeCP2 (Abcam) and monoclonal HDAC1 (Abcam) (n = 3). Data represent mean ± SEM. *, $P = .01$ (GR:HDAC1); .003 (GR: MeCP2); .027 (MeCP2: HDAC1). A.U., arbitrary units; ab, antibody; IP, immunoprecipitation; Veh, vehicle; WB, Western blot.

suggest that Dex treatment leads to the formation of a complex containing GR, MeCP2, and HDAC1.

Dex increases GR, MeCP2, HDAC1, and DnMT3b occupancy in the region of the crh promoter

In keeping with the coimmunoprecipitation data (Figure 3) and previously reported ChIP data (12), Dex exposure increased GR occupancy in the region of the *crh* proximal promoter (Figure 4, A and B); however, GR occupancy was not detected in farther upstream regions

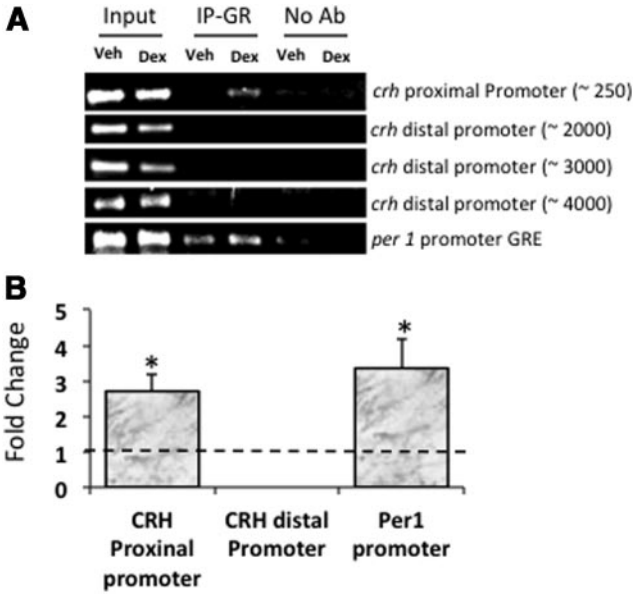

Figure 4. Dex Treatment Induces the Recruitment of GR to the *crh* Proximal Promoter. A, Representative gel images of amplicons. B, Fold change over vehicle (set as 1, dashed line). Cells were treated as in Figure 1, and ChIP was performed with a monoclonal antibody against GR (Thermo/Pierce). Real-time PCR was performed using primers targeted to the *crh* or *per1* promoter (n = 3). Bars represent the mean ± SEM and are represented as the fold difference of the vehicle (Veh). *, $P = .01$ (*crh*); .005 (*Per1*). Ab, antibody; IP, immunoprecipitation.

of the *crh* promoter (−4000 through −2000) (Figure 4, A and B), indicating specificity to the site of GR occupancy. GR is known to positively regulate the period circadian protein homolog 1(Per1) gene through a GRE. Therefore, as a positive control, GR occupancy was assessed at the *per1* promoter. Dex led to 3- to 4-fold increase of GR at the *per1* promoter (Figure 4, A and B). Furthermore, unlike *per1* occupancy, GR occupancy at the *crh* promoter is undetectable in the absence of Dex. Thus, our findings are specific to GR recruitment to the proximal *crh* promoter.

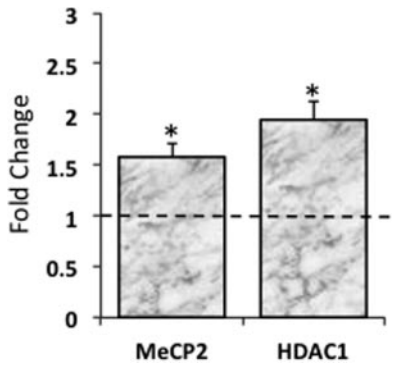

Figure 5. Dex Treatment Induces Recruitment of HDAC1 and MeCP2 to the *crh* Promoter. ChIP analysis was performed with a monoclonal antibody against HDAC1 (Abcam) or MeCP2 (Sigma). The data are expressed as fold vehicle (dashed line) (n = 3). Data represent mean ± SEM. *, $P = .01$(MeCP2); .001 (HDAC1).

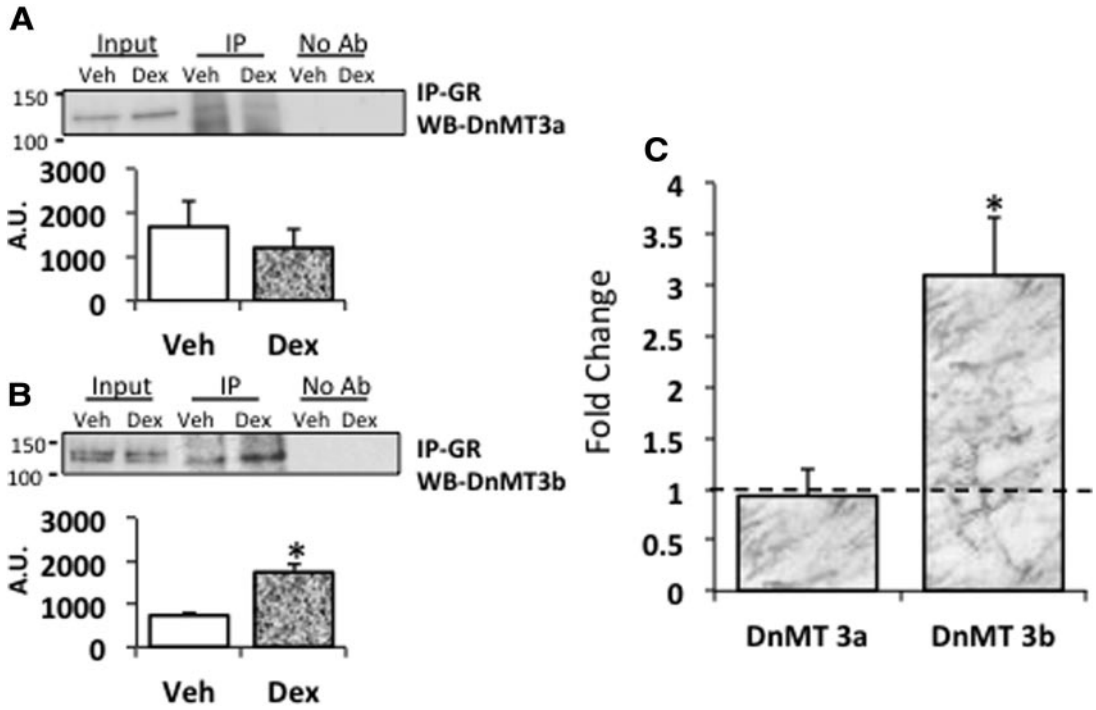

Figure 6. Dex Induces GR Interaction with DnMT3b and Its Recruitment to the Region of the *crh* Promoter. A and B, Coimmunoprecipitation analysis of GR-DnMT3a and -3b interactions. C, ChIP analysis of DnMT3a and -3b. Antibodies used were monoclonal GR (Thermo/Pierce), DnMT3a and -3b (Santa Cruz) (n = 3). Bars represent the mean ± SEM and are represented as the fold difference of the Veh. *, .011 (GR:DnMT3b); .009 (DnMT3b Chip). A.U., arbitrary units; ab, antibody; IP, immunoprecipitation; Veh, vehicle; WB, Western blot.

Given the coimmunoprecipitation results that GR associates with HDAC1 and MeCP2, and that HDAC1 and MeCP2 interact with each other (Figure 3), ChIP analyses were performed to assess the effect of Dex treatment on MeCP2 and HDAC1 occupancy. Dex treatment was associated with significantly increased HDAC1 and MeCP2 occupancy at the *crh* promoter (Figure 5). Taken together, the coimmunoprecipitation and ChIP data are consistent with the formation of a Dex-induced GR-MeCP2-HDAC1 repressive complex that targets the *crh* proximal promoter.

Dex induces GR-DnMT3b interactions and DnMT3b occupancy in the region of the crh promoter

Given that MeCP2 binds to methylated CpG dinucleotides and DnMTs are involved in such methylation (37), we sought to determine whether or not DnMTs associate with the GR and/or are present in the same region of the *crh* proximal promoter as evaluated above. An interaction between GR and DnMT3a was not observed. The bands in Figure 6A, IP, are not specific. In contrast, GR interacted with DnMT3b, and the interaction was increased by treatment with Dex (Figure 6B). By ChIP analysis, DnMT3a and 3b were present in the region of the *crh* promoter; however, Dex increased DnMT3b occupancy only (Figure 6C). Thus, GR interacts only with DnMT3b, and Dex increases DnMT3b *crh* occupancy, specifically.

Dex increases crh promoter methylation at specific CpG sites

To determine whether the recruitment of DnMT3b was associated with its function as a CpG methyltransferase, the degree of CpG methylation in the proximal promoter region was measured by sodium bisulfite sequencing. Analysis of methylation levels over all the 11 CpG sites present in this region (Figure 7A) revealed a significant increase in the average percentage of methylation after Dex treatment (Figure 7, B and C). Further analysis revealed that methylation was site specific. Only 2 of the 11 sites assessed displayed an increase in methylation level after Dex treatment. These were at −34 and −36 (CpG no. 9 and 10; Figure 7D). The CpG present at −147 (site 4) was constitutively hypomethylated. Thus, Dex induces site-specific CpG methylation at the *crh* proximal promoter.

Dex increases the methylation of H3-K9 in the region of the *crh* promoter

In addition to DNA methylation, specific histone modifications are associated with repressed chromatin. Indeed histone modifications have been shown to act together

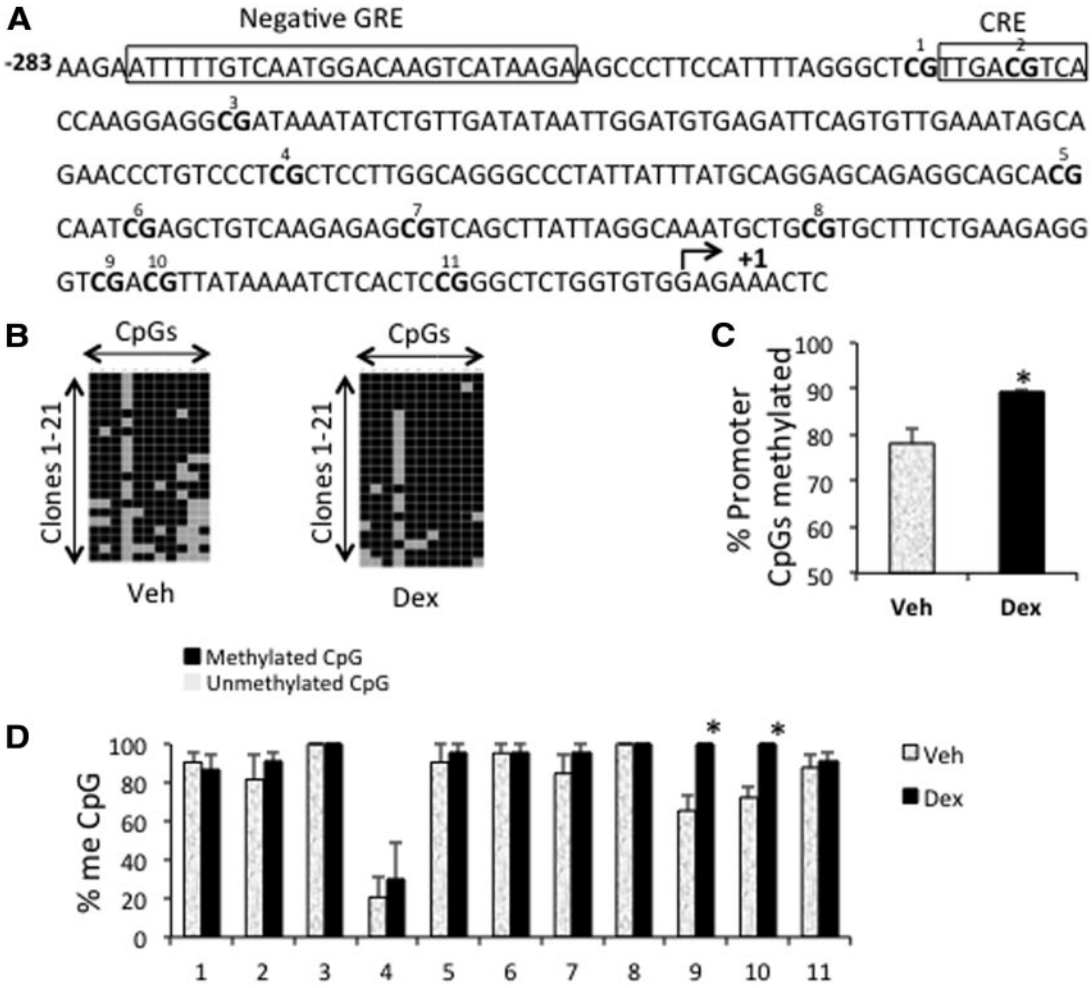

Figure 7. Dex Increases *crh* Promoter Methylation at Specific CpG Sites. A, Sequence of rat *crh* promoter. Small numbers indicate the methylation sites in the proximal promoter. The arrow indicates the transcriptional start site. B, Raw sequencing data for promoter methylation. Each row represents an independent clone. C, Analysis of overall methylation across all sites. D, Percent methylation at specific sites. Analysis of *crh* promoter DNA methylation was performed by sequencing of PCR clones derived from sodium bisulfite- treated genomic DNA (n = 3). Bars represent the mean ± SEM. *, $P = .05$. Veh, vehicle.

with DNA methylation to repress gene transcription (24). We previously assessed acetylation in this region of the *crh* proximal promoter by ChIP analysis (12). Here, we sought to determine whether or not Dex would induce changes in specific methylation marks in this region. H3-K9 exists in 3 methylation states: mono-, di-, and tri- (38). Chromatin was immunoprecipitated with an antibody that detects all 3 states of H3-K9 methylation, and Dex treatment led to an increase in overall methylation of H3-K9 (Figure 8). ChIPs were also performed to determine the effect of Dex on the degree of di- or trimethylation. As shown in Figure 8, Dex increased the H3-K9 tri-, but, not di-methylated, level. Lastly, we assessed the methylation of the lysine 4 residue of histone H3 (H3-K4), which in the trimethylated state has been shown to be a marker for gene activation. Dex failed to alter levels of di- or trimethylated H3-K4 (Figure 8). Thus, Dex increased methylation of residues associated with repression but not activation.

Discussion

Taken together, the data suggest that a GR-HDAC1-MeCP2 repressor complex participates in Dex-mediated *crh* down-regulation. Recruitment of this complex occurs in parallel with GR interaction with DnMT3b and its recruitment to the *crh* proximal promoter. Whether or not DnMT3b is physically associated with the GR-HDAC1-MeCP2 complex remains to be determined. The recruitment of DnMT3b is functional in so far as its presence occurs in parallel with site-specific promoter methylation. Lastly, specific histone methylation also appears to play a part in *crh* down-regulation: Dex treatment leads to an increase in tri-methylated H3-K9.

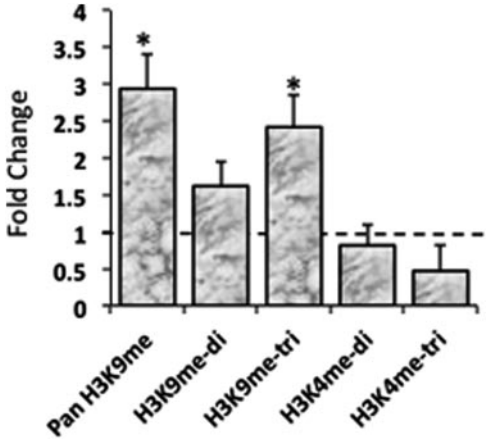

Figure 8. Dex Increases Trimethylation of H3–K9. ChIP analysis of histone H3–K9 and H3–K4 methylation. The antibodies used are polyclonal Pan H3–K9 (Active Motif), polyclonal trimethyl H3–K9 (Abcam), monoclonal di- and trimethyl H3–K4 and dimethyl H3–K9 (n = 3). Data are presented as the mean ± SEM and are represented as the fold of Veh (dashed line). *, $P = .009$ (Pan H3K9); .01 (H3K9-di); .01(H3K9-tri)

The vast majority of studies designed to elucidate glucocorticoid effects on hypothalamic *crh* expression have examined involvement of the CRE and nGRE in the CRH proximal promoter. With respect to mechanisms that involve recruitment of negative regulatory proteins, we previously reported that Dex-associated suppression of CRH mRNA levels correlates with increased HDAC1 at the proximal *crh* promoter (12). Consistent with HDAC1's ability to bind MeCP2 (16), and reports of HDAC1-DnMT3b interactions (39), we observed an increased recruitment of HDAC1, MeCP2, and DnMT3b at the promoter. Based on the results of this study and earlier reports, in all likelihood the GR holoreceptor induces decreased *crh* transcription via formation of one or more repressor complexes recruited to the proximal *crh* promoter.

The requirements for each of these proteins for Dex-mediated repression and the order in which they associate and/are recruited to the region of the promoter have yet to be determined. One scenario would involve GR-DNA binding (Figure 9A). A glucocorticoid-bound GR would be recruited to the nGRE. The GR holoreceptor would then recruit DnMT3b to the promoter region, which would methylate specific CpG sites. GR would then recruit and/or stabilize MeCP2 binding to the meCpG docking sites. Either GR or MeCP2 could recruit HDAC1, and the resulting complex would lead to down-regulated gene expression. Another scenario does not involve direct GR-DNA binding (Figure 9B). In this case, MeCP2 bound to meCpG sites would recruit GR, the GR might stabilize HDAC1 interactions with MeCP2 and then, as in the first scenario (Figure 9A), HDAC1 would lead to altered expression of *crh* (Figure 9B). In this scenario a GR-DnMT3b complex could be independent of a GR-MeCP2- HDAC1 complex (Figure 9B). Alternatively, it could be part of the GR-MeCP2-HDAC1 complex in that DnMT3b-HDAC1 interactions have been reported (39).

Although mechanisms for Dex-increased H3-K9 trimethylation cannot be based on data presented here, it is known that Suv39H1 methylates H3-K9 (40). Thus, it may be that this methylase directly or indirectly interacts with the GR to modify H3-K9 methylation status. Indeed, Suv39h interacts with DNMT3b and HDAC1 (41). Furthermore, there is precedent for Suv39H1 playing a role in repression of transcription factor activity. For example, it interacts with the transcription factor Smad5 to repress transcription (42).

To date, there are 3 reports of systematic analyses of the *crh* promoter that focus on events that involve MeCP2 binding and/or methylation (17–19). McGill et al. showed that the HPA axis activity of mice bearing an MeCP2 mutation is refractory to glucocorticoid down-regulation. This dysfunction was independent of the degree of levels of CpG methylation in that the degree of methylation in the mutant mouse is the same as in wild type. Dysfunction was associated with the degree of MeCP2 promoter binding in the region of the *crh* proximal promoter. In the wild-type mice, sequential ChIP analysis of the proximal *crh* promoter mapped the site of greatest binding to the region surrounding the proximal CRE (−226). In mutant mice there was no binding.

In the context of in vivo stress models, Elliott et al. (19) and Chen et al. (18) revealed that methylation of specific sites in the promoter were altered. In both cases the stressor induced hypomethylation within the CRE (site 2 in the Chen report and in the numbering system used here). Stressors increased *crh* expression and decreased methylation in the region of the proximal CRE, in keeping with functional pCREB binding.

The data presented here contrast with those presented by Elliott et al and Chen et al. Here, there was no alteration in the degree of methylation in the region of the CRE. Rather, Dex increased methylation at −36 and −33 (sites 9 and 10 as presented here). Interestingly, in both mice reports, the CpG at −36 is the most hypomethylated site in the regions examined (17, 19). In the mouse reports, data for position −33 (site 10) are not reported, consistent with one of the few species-specific sequence differences in the proximal promoter: the site is a CG in rat but a CA in mouse. In rat, data for sites 9 and 10 were not reported (18).

In data shown here, from cells derived from rat, the singularly most hypomethylated position is −147 (site number 4). Site 4 is also hypomethylated in rat in vivo but

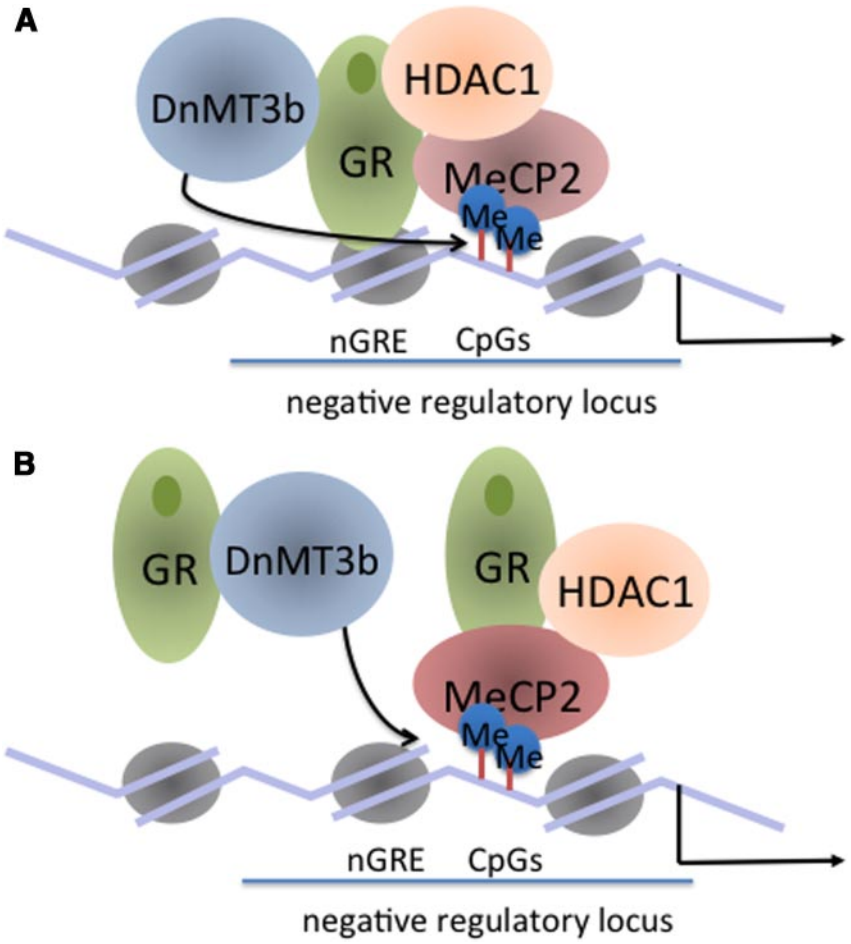

Figure 9. Models of GR-Mediated *crh* Down-Regulation. A, A DNA binding-dependent mechanism. A, GR holoreceptor monomer binds to the nGRE and recruits DnMT3b. DnMT3b methylates the promoter and subsequently leads to the recruitment of MeCP2. GR and/or MeCP2 recruit HDAC1. The assembled then represses *crh* expression. B, A DNA binding-independent mechanism. A GR holoreceptor bound or not bound to MeCP2 associates with DnMT3b. A GR-MeCP2-HDAC1, assembles at the promoter. The order of recruitment and assembly are not known. Me, methyl; MeCP2, Methyl CpG binding protein 2.

not uniquely so (18). The degree of methylation both at sites 9 (−36) in mouse and 4 (−147) in rat are refractory to experimental manipulation. The role of persistently hypomethylated sites in this context has not been explored. It may be that they are required for stabilizing species-specific activating proteins.

One explanation for the difference in methylation patterns between the stress (18, 19) and nonstress models (17) could be that Dex-mediated repression of *crh* basal activity occurs through a fundamentally different mechanism than does reversal of a response to a stimulus. In the wild-type quiescent state (17), MeCP2 is present at the CRE. This is in accord with the data presented here in which Dex increases recruitment of MeCP2, DnMTb, and methylation at the *crh* promoter-proximal promoter. The reversal to a response to a stimulus includes the inducible cAMP early repressor of the CREB family (Ref. 13 for review). It would be interesting to determine the interaction of inducible cAMP early repressor with the proteins examined here.

Although the focus of this report has been to elucidate molecular mechanisms by which the GR closes the negative feedback loop in the neuroendocrine component of the HPA axis, elucidating these mechanisms also has implications for understanding neuropsychiatric behavior. Abnormal HPA axis regulation is tightly correlated with depression (43, 44). For example, depressed individuals are unable to down-regulate cortisol levels in response to Dex as administered in the Dex suppression test (45). Elliott et al (19) assessed epigenetic contributions to *crh* regulation in the context of the social avoidance model of depression. The authors showed that the changes in CpG methylation were associated with social avoidance. Remarkably, these changes were diminished by administration of imipramine, a widely used antidepressant. Functional integration of methylation at the 2 different regions of the promoter will be important to determine in a species-specific manner, and one in which stressors and glucocorticoids are both manipulated. Such studies may ultimately reveal mechanisms by which chromatin modifications and epigenetic regulation lead to individual differences in the stress response and the development of depressive behaviors.

Acknowledgments

Address all correspondence and requests for reprints to: Rosalie M. Uht, Institute for Aging and Alzheimer's Disease, Department of Pharmacology & Neuroscience, University of North Texas Health Science Center, CBH 469, 3500 Camp Bowie Boulevard, Fort Worth, Texas 76107. E-mail: rosalie.uht@unthsc.edu.

This work was supported by National Institutes of Health Grant R01-MH082900 (to R.M.U.). Part of the data in this report was presented at the 2012 Endocrine Society Meeting, for which the presenter (S.B.) received an Outstanding Abstract Travel Award.

Current address for D.S.: School of Natural Sciences & Math, University of Texas at Dallas, Dallas, Texas.

Disclosure Summary: The authors have nothing to disclose.

References

1. **Vale W, Rivier C, Brown MR, et al.** Chemical and biological characterization of corticotropin releasing factor. *Recent Prog Horm Res*. 1983;39:245–270.
2. **Rivier C, Rivier J, Vale W.** Inhibition of adrenocorticotropic hormone secretion in the rat by immunoneutralization of corticotropin-releasing factor. *Science*. 1982;218:377–379.
3. **Watts AG.** Glucocorticoid regulation of peptide genes in neuroendocrine CRH neurons: a complexity beyond negative feedback. *Front Neuroendocrinol*. 2005;26:109–130.
4. **Beyer HS, Matta SG, Sharp BM.** Regulation of the messenger ribonucleic acid for corticotropin-releasing factor in the paraventricular nucleus and other brain sites of the rat. *Endocrinology*. 1988;123:2117–2123.
5. **Jingami H, Matsukura S, Numa S, Imura H.** Effects of adrenalectomy and dexamethasone administration on the level of preprocorticotropin-releasing factor messenger ribonucleic acid (mRNA) in the hypothalamus and adrenocorticotropin/β-lipotropin precursor mRNA in the pituitary in rats. *Endocrinology*. 1985;117:1314–1320.
6. **Seasholtz AF, Thompson RC, Douglass JO.** Identification of a cyclic adenosine monophosphate-responsive element in the rat corticotropin-releasing hormone gene. *Mol Endocrinol*. 1988;2:1311–1319.
7. **Spengler D, Rupprecht R, Van LP, Holsboer F.** Identification and characterization of a 3′,5′-cyclic adenosine monophosphate-responsive element in the human corticotropin-releasing hormone gene promoter. *Mol Endocrinol*. 1992;6:1931–1941.
8. **Malkoski SP, Dorin RI.** Composite glucocorticoid regulation at a functionally defined negative glucocorticoid response element of the human corticotropin-releasing hormone gene. *Mol Endocrinol*. 1999;13:1629–1644.
9. **Wölfl S, Martinez C, Majzoub JA.** Inducible binding of cyclic adenosine 3′,5′-monophosphate (cAMP)-responsive element binding protein (CREB) to a cAMP-responsive promoter in vivo. *Mol Endocrinol*. 1999;13:659–669.
10. **Nikodemova M, Kasckow J, Liu H, Manganiello V, Aguilera G.** Cyclic adenosine 3′,5′-monophosphate regulation of corticotropin-releasing hormone promoter activity in AtT-20 cells and in a transformed hypothalamic cell line. *Endocrinology*. 2003;144:1292–1300.
11. **Malkoski SP, Handanos CM, Dorin RI.** Localization of a negative glucocorticoid response element of the human corticotropin releasing hormone gene. *Mol Cell Endocrinol*. 1997;127:189–199.
12. **Miller L, Foradori CD, Lalmansingh AS, Sharma D, Handa RJ, Uht RM.** Histone deacetylase 1 (HDAC1) participates in the downregulation of corticotropin releasing hormone gene (crh) expression. *Physiol Behav*. 2011;104:312–320.
13. **Aguilera G, Liu Y.** The molecular physiology of CRH neurons. *Front Neuroendocrinol*. 2012;33:67–84.
14. **Bestor TH, Verdine GL.** DNA methyltransferases. *Curr Opin Cell Biol*. 1994;6:380–389.
15. **Comb M, Goodman HM.** CpG methylation inhibits proenkephalin gene expression and binding of the transcription factor AP-2. *Nucleic Acids Res*. 1990;18:3975–3982.
16. **Nan X, Ng HH, Johnson CA, et al.** Transcriptional repression by the methyl-CpG-binding protein MeCP2 involves a histone deacetylase complex. *Nature*. 1998;393:386–389.
17. **McGill BE, Bundle SF, Yaylaoglu MB, Carson JP, Thaller C, Zoghbi HY.** Enhanced anxiety and stress-induced corticosterone release are associated with increased Crh expression in a mouse model of Rett syndrome. *Proc Natl Acad Sci USA*. 2006;103:18267–18272.
18. **Chen J, Evans AN, Liu Y, Honda M, Saavedra JM, Aguilera G.** Maternal deprivation in rats is associated with corticotrophin-releasing hormone (CRH) promoter hypomethylation and enhances CRH transcriptional responses to stress in adulthood. *J Neuroendocrinol*. 2012;24:1055–1064.
19. **Elliott E, Ezra-Nevo G, Regev L, Neufeld-Cohen A, Chen A.** Resilience to social stress coincides with functional DNA methylation of the Crf gene in adult mice. *Nat Neurosci*. 2010;13:1351–1353.
20. **Noma K, Allis CD, Grewal SI.** Transitions in distinct histone H3 methylation patterns at the heterochromatin domain boundaries. *Science*. 2001;293:1150–1155.
21. **Litt MD, Simpson M, Gaszner M, Allis CD, Felsenfeld G.** Correlation between histone lysine methylation and developmental changes at the chicken β-globin locus. *Science*. 2001;293:2453–2455.
22. **Santos-Rosa H, Schneider R, Bannister AJ, et al.** Active genes are tri-methylated at K4 of histone H3. *Nature*. 2002;419:407–411.
23. **Saccani S, Natoli G.** Dynamic changes in histone H3 Lys 9 methylation occurring at tightly regulated inducible inflammatory genes. *Genes Dev*. 2002;16:2219–2224.
24. **Fuks F.** DNA methylation and histone modifications: teaming up to silence genes. *Curr Opin Genet Dev*. 2005;15:490–495.
25. **Kasckow J, Mulchahey JJ, Aguilera G, et al.** Corticotropin-releasing hormone (CRH) expression and protein kinase A mediated CRH receptor signalling in an immortalized hypothalamic cell line. *J Neuroendocrinol*. 2003;15:521–529.
26. **Livak KJ, Schmittgen TD.** Analysis of relative gene expression data using real-time quantitative PCR and the 2(-Δ Δ C(T)) Method. *Methods*. 2001;25:402–408.
27. **Sadowski HB, Gilman MZ.** Cell-free activation of a DNA-binding protein by epidermal growth factor. *Nature*. 1993;362:79–83.
28. **Towbin H, Staehelin T, Gordon J.** Electrophoretic transfer of proteins from polyacrylamide gels to nitrocellulose sheets: procedure and some applications. *Proc Natl Acad Sci USA*. 1979;76:4350–4354.
29. **Chakrabarti SK, James JC, Mirmira RG.** Quantitative assessment of gene targeting in vitro and in vivo by the pancreatic transcription factor, *Pdx1*. Importance of chromatin structure in directing promoter binding. *J Biol Chem*. 2002;277:13286–13293.
30. **Lalmansingh AS, Uht RM.** Estradiol regulates corticotropin-releasing hormone gene (crh) expression in a rapid and phasic manner that parallels estrogen receptor-α and -β recruitment to a 3′,5′-cyclic adenosine 5′-monophosphate regulatory region of the proximal crh promoter. *Endocrinology*. 2008;149:346–357.
31. **Sharma D, Handa RJ, Uht RM.** The ERβ ligand 5α-androstane, 3β,17β-diol (3β-diol) regulates hypothalamic oxytocin (Oxt) gene expression. *Endocrinology*. 2012;153:2353–2361.
32. **Kriaucionis S, Bird A.** The major form of MeCP2 has a novel N-terminus generated by alternative splicing. *Nucleic Acids Res*. 2004;32:1818–1823.
33. **Mnatzakanian GN, Lohi H, Munteanu I, et al.** A previously unidentified MECP2 open reading frame defines a new protein isoform relevant to Rett syndrome. *Nat Genet*. 2004;36:339–341.
34. **Dastidar SG, Bardai FH, Ma C, et al.** Isoform-specific toxicity of Mecp2 in postmitotic neurons: suppression of neurotoxicity by FoxG1. *J Neurosci*. 2012;32:2846–2855.
35. **Meehan RR, Lewis JD, Bird AP.** Characterization of MeCP2, a vertebrate DNA binding protein with affinity for methylated DNA. *Nucleic Acids Res*. 1992;20:5085–5092.
36. **Kim JY, Shen S, Dietz K, et al.** HDAC1 nuclear export induced by pathological conditions is essential for the onset of axonal damage. *Nat Neurosci*. 2010;13:180–189.
37. **Wade PA.** Methyl CpG binding proteins: coupling chromatin architecture to gene regulation. *Oncogene*. 2001;20:3166–3173.

38. **Lachner M, Jenuwein T.** The many faces of histone lysine methylation. *Curr Opin Cell Biol*. 2002;14:286–298.
39. **Geiman TM, Sankpal UT, Robertson AK, Zhao Y, Zhao Y, Robertson KD.** DNMT3B interacts with hSNF2H chromatin remodeling enzyme, *HDACs 1 and 2*, and components of the histone methylation system. *Biochem Biophys Res Commun*. 2004;318:544–555.
40. **Rea S, Eisenhaber F, O'Carroll D, et al.** Regulation of chromatin structure by site-specific histone H3 methyltransferases. *Nature*. 2000;406:593–599.
41. **Fuks F, Hurd PJ, Deplus R, Kouzarides T.** The DNA methyltransferases associate with HP1 and the SUV39H1 histone methyltransferase. *Nucleic Acids Res*. 2003;31:2305–2312.
42. **Frontelo P, Leader JE, Yoo N, et al.** Suv39h histone methyltransferases interact with Smads and cooperate in BMP-induced repression. *Oncogene*. 2004;23:5242–5251.
43. **Holsboer F, Barden N.** Antidepressants and hypothalamic-pituitary-adrenocortical regulation. *Endocr Rev*. 1996;17:187–205.
44. **Nemeroff CB, Vale WW.** The neurobiology of depression: inroads to treatment and new drug discovery. *J Clin Psychiatr*. 66(Suppl 7):5–13.
45. **Carroll BJ, Feinberg M, Greden JF, et al.** A specific laboratory test for the diagnosis of melancholia. Standardization, validation, and clinical utility. *Arch Gen Psychiatry*. 1981;38:15–22.